Influence of wave aberrations on MTF measurements modelled by the pupil function

Markus Schake, Hanno Dierke
Physikalisch-Technische Bundesanstalt, Bundesallee 100, 38116 Braunschweig, Germany
mailto:markus.schake@ptb.de

This article discusses different approaches to model the influence of wave aberrations on the modulation transfer function (MTF) by the complex pupil function. Numerical propagation of Huygens' elementary waves, the solution of the Fraunhofer approximation and a Fourier optical method are compared.

1 Introduction

When light passes through a system of optical components, each of them will cause a certain phase transformation depending on its form and refractive index. The point spread function (PSF) of an optical system may be modelled as the Fraunhofer diffraction pattern of its complex pupil function, which, including all multiplicative phase transformations acquired while passing the system, finally emerges from the exit pupil [1, 2]. For a diffraction limited system, the wavefront at the exit pupil is assumed to be illuminated by a perfectly spherical wave. In the presence of aberrations, these are modelled as additional wavefront form errors in the complex pupil function. The application of the complex pupil function to describe errors in the PSF is applied in [3] in the context of image restoration. In [4], measured edge spread functions are employed to retrieve the Zernike coefficients of wavefront aberrations in the complex pupil function by solving an inverse problem. In this contribution different simulation methods are employed to demonstrate the influence of different wavefront errors modelled by Zernike polynomials on the PSF and its associated MTF. The results will be employed in the estimation of the measurement uncertainty in the multi camera MTF measurement setup at PTB [5].

2 Simulation models

This section shortly introduces the different methods used to simulate the PSF or line spread function (LSF) in dependence of the complex pupil function of the sample under test. In the scope of this work only rectangular apertures and detectors are considered, however all methods presented here may also be applied to circular apertures.

Wave propagation by Huygens' elementary waves:

Each point (x, y, z) in the x-y-aperture plane is modelled as the source of a spherical elementary wave of amplitude $A(x, y)$, wavelength λ and wave vector $k = \frac{2\pi}{\lambda}$ propagating to a point (p_x, p_y, p_z) in the detector plane along the radial vector $r = \sqrt{((p_x - x)^2 + (p_y - y)^2 + (p_z - z))^2}$ [2]. The electric field of the elementary waves is described by Eq. (1), with $W(x, y)$ being the phase distribution associated with the wavefront aberration in the aperture plane.

$$U = \frac{A(x, y)}{r} \cdot e^{-ik(r+W(x,y))} \tag{1}$$

The electric field on the detector results from the superposition of all elementary waves.

$$U_s = \sum_x \sum_y U(x, y, p_x, p_y, p_z - z) \tag{2}$$

The calculation of the field on the detector with this method is impractical for high numbers of sample points due to its high computational load. Thus, this method is only considered here for 1D profiles in the aperture plane.

Analytical solution for the rectangular aperture:

For the case of a rectangular aperture of dimension w_x, w_y and an incoming plane wave, an analytical solution of the Fraunhofer integral exists [2]. The diffraction limited field distribution on the detector is given by Eq. (3).

$$U_s = \frac{A}{\lambda(p_z - z)} \text{sinc}(\frac{2w_x p_x}{\lambda(p_z - z)}) \text{sinc}(\frac{2w_y p_y}{\lambda(p_z - z)}) \tag{3}$$

The analytical solution may be adjusted to cover defocus effects, however it is not applicable for arbitrary wavefront aberrations in the aperture plane and only considers a homogenous and constant intensity distribution A.

Numerical solution of the Fraunhofer integral

As stated in [1], the solution of the Fraunhofer integral in the focus plane of a lens is given by Eq. (4).

$$U_s = C \sum_x \sum_y A(x, y) e^{-ik(xp_x + yp_y + W(x,y))} \tag{4}$$

Here C describes the scaling of the amplitude. Eq. (4) shows some similarity to Eq. (2) for the Huygens' elementary waves. It is noteworthy however, that since the solution of Eq. (4) is confined to the focal plane of the lens its propagation along the radial distance r is not explicitly calculated, which saves a lot of computational effort.

Fourier optical approach

The solution of the Fraunhofer integral in the focus plane of a lens, which represents the far field diffrac-

DGaO Proceedings 2023 – http://www.dgao-proceedings.de – ISSN: 1614-8436 – urn:nbn:de:0287-2023-B044-8
submitted: 20.07.2023 – published: 21.08.2023

tion image of the complex pupil function in the aperture, may also be determined by Fourier transformation of the complex pupil function [2, 3]. The electric field in the aperture plane who's amplitude and phase distribution are defined by the complex pupil function is defined in Eq. (5).

$$U = A(x,y)e^{-ikW(x,y)} \tag{5}$$

The lateral sampling distance in the aperture plane d_x, d_y, the focal distance of the modelled lens f and the number of samples in each direction N_x, N_y are required to determine the correct scaling in the image plane, where the diffraction pattern is observed. The lateral spacing in the image plane is defined as

$$d_{px} = \frac{f\lambda}{N_x d_x},\ d_{py} = \frac{f\lambda}{N_y d_y}. \tag{6}$$

The field in the image plane is calculated employing

$$U_s = \frac{A(x,y)}{\lambda f}\left|\mathrm{FFT}\left(U(x,y)\right)\right|. \tag{7}$$

As for the numerical solution of the Fraunhofer integral, this method is also confined in its applicability to the focal plane of the lens.

Since the intensity is proportional to the square of the electric field, the results of Eq. (2), (3), (4) and (7) are squared to determine the intensity distribution in the image plane.

3 Results and conclusions

To test and compare the different approaches, the diffraction image of a spherical lens with focal length $f = 50\,\mathrm{mm}$ and quadratic aperture diameter $D = 5\,\mathrm{mm}$ is considered at a wavelength of $\lambda = 546\,\mathrm{nm}$. In the case of a plane input wavefront all simulation methods yield similar results. The numerical methods show a higher deviation to the diffraction limited MTF than the FFT method due to their low number of sampling points in the aperture plane, which is used to decrease simulation time. To get an impression of the impact of wavefront errors on the MTF a trefoil error has been added to the plane input wavefront by setting the Zernike coefficient $Z_3^3 = -2 \cdot 10^{-6}\,\mathrm{mm}$. The MTF deviations caused by the trefoil as predicted by the different simulation methods are depicted in Fig. 1. The analytical model (blue diamonds) does not incorporate the wavefront aberration. The 1D approaches (orange crosses and yellow circles) only consider a cut through the input aperture and do not correctly represent the influence of the trefoil error on the MTF. The LSF approaches (solid violett line and dashed green line) are based on a 2D modelling of the wavefront aberration and yield the best representation of the MTF deviation caused by the trefoil error. The difference between the Fraunhofer (solid violet line) and the FFT (dashed green line) approach is caused by the rather low spatial resolution employed in the numerical solution of the Fraunhofer integral. Increased resolution causes these results to converge but greatly increases the computation time. In conclusion the Fourier optical approach of Fourier transforming the complex pupil function to yield the diffraction pattern is the fastest implementation and yields the best result since it allows higher resolution in the spatial sampling.

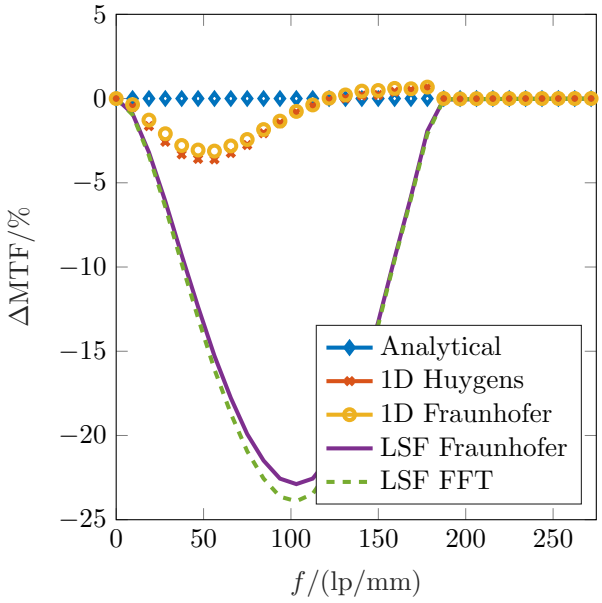

Fig. 1 *Difference between the ideal diffraction limited MTF and the MTF obtained for the wavefront with peak to valley trefoil error of* $400\,\mathrm{nm}$.

To get a better understanding and hands-on experience with the influence of wavefront errors on the MTF the reader is referred to our simulation data which is provided open access via the PTB's open access repository under the citable DOI: 10.7795/710.20230628 [6]. The software allows to simulate and evaluate arbitrary wavefront error combinations based on Zernike polynomials for rectangular aperture planes.

References

[1] M. Born and E. Wolf, *Principles of optics*, 6th ed. (Pergamon Press, New York, 1980).

[2] J. W. Goodman, *Introduction to Fourier Optics*, 2nd ed. (McGraw Hill, New York, 1996).

[3] P. Mueller, M. Lehmann, and A. Braun, "Optical quality metrics for image restoration," in *Digital Optical Technologies 2019*, B. C. Kress and P. Schelkens, eds., vol. 11062, p. 1106214, International Society for Optics and Photonics (SPIE, 2019). URL `https://doi.org/10.1117/12.2528100`.

[4] S. Kraemer and T. Sure, "Experimentelle Bestimmung von Zernike-Koeffizienten anhand gemessener Kantenbildfunktionen," in *DGAO Proceedings*, vol. 122 A3, DGAO (DGAO, 2021). URL `https://www.dgao-proceedings.de/download/122/122_a3.pdf`.

[5] M. Schake and M. Schulz, "Identification of aliasing effects in measurements of unknown MTFs," in *Optical Metrology and Inspection for Industrial Applications VIII*, S. Han, G. Ehret, and B. Chen, eds., vol. 11899, pp. 67 – 80, International Society for Optics and Photonics (SPIE, 2021). URL `https://doi.org/10.1117/12.2601176`.

[6] M. Schake, "Simulation tool for "Influence of wave aberrations on MTF measurements modelled by the pupil function"," (PTB, 2023). URL `https://oar.ptb.de/resources/show/10.7795/710.20230628`.